Journal of Electrical and Computer Engineering Innovations
(JECEI)
Journal homepage: http://www.jecei.sru.ac.ir

Research paper

Frequency and Voltage Control of an Inverter-Based DG Using Adaptive Fuzzy-Sliding Mode Controller

E. Limouchi, S.A. Taher, B. Ganji*

Faculty of Electrical and Computer Engineering, University of Kashan, Kashan, Iran.

Article Info

Article History:
Received 01 September 2018
Reviewed 11 November 2018
Revised 07 February 2019
Accepted 17 April 2019

Keywords:
Microgrid
Distributed generation
Frequency control
voltage control

*Corresponding Author's Email Address:
bganji@kashanu.ac.ir

Abstract

Background and Objectives: The microgrid voltage and frequency are strongly affected by active and reactive load fluctuations. Load change in microgrid may result in the lack of balance among generation and consumption and as a result change in output voltage and frequency. If load change is great enough, distribution generation cannot stabilize the microgrid. The main objective of this article is to control the distribution of active and reactive power related to an inverter-based distributed generation (DG) in the microgrid using intelligent methods.
Methods: In this study, frequency and voltage of an active generator connected to the microgrid is also controlled with applying adaptive the fuzzy sliding mode control (AFSMC) and the droop control Methods To solve the problems related to design of the sliding mode controller, a compensator control system is suggested. A rule based on the Lyapunov stability theory is also introduced to ensure the stability of closed loop system.
Results: Using MATLAB/SIMULINIK software, simulation results are provided for the proposed controller and its performance under different conditions for a typical power system is evaluated. Simulation of the considered power system is done to track different values of active and reactive power.
Conclusion: The provided simulation results show the effectiveness of suggested method to regulate active and reactive power and to control voltage and frequency of the microgrid.

Introduction

Recently, microgrid and distributed generation (DG) are two well-known concepts in the power distribution system. The microgrid is collection of distribution generations which work together for safe and economic power transmission. Some new challenges about operation of microgrid and control of voltage and frequency are presented in [1]-[3] . The effects of energy storage tools on microgrid dynamic response are studied in [4]. To regulate voltage and frequency of microgrid in connected mode, direct-quadrature current control method is proposed in [5]-[6]. To improve the performance and the stability of the power system, various control methods are usually introduced [7]. A disturbance observer method is used in [8] to overcome the weaknesses of droop control strategy for load sharing and voltage stability in a DC microgrid. For control of power system, the intelligent algorithms such as artificial neural networks (ANN) are also used frequently [9][10]. In [11], ANN is used to assess voltage stability. Using intelligent techniques such as fuzzy logic (FL) and ANNs, control of power systems is reported in [12]. Despite multiple advantages, microgrid leads to new problems such as change of power flow pattern, increase of high frequency harmonics due to using inverter-based DG, and increasing frequency and voltage fluctuations resulted from the changing nature of renewable energy sources [13]. Renewable energy sources are usually connected to microgrid by power electronic interfaces such as inverters. In islanding mode of microgrid, voltage source inverter (VSI) is used more [14]. In this case, microgrid frequency and voltage are controlled through local control loops. To avoid from flow circulation among parallel inverters connected to microgrid, control strategies based on droop characteristic are usually applied [15]. Different methods are recommended to control inverters output power along with power management in past years. Many researchers have also worked on design of controller. For instance, proportional-integral controller (PI) in [16]-[17], proportional resonance in [18][19], fuzzy control in [20]-[21] and predictive control in[22]-[23] can be observed. The conventional PI is a simple controller with easy performance but it is so sensitive to change of the system parameters. In addition, PI regulation is complex. One way to control active power of the generator is the sliding mode control that has a high speed in compared with PI. The sliding mode control is a robust method which is effective in uncertainties and external disturbances [24]. At the time of microgrid islanding, appropriate control structure is required to achieve objectives such as voltage and frequency control [25]. The reduction of total harmonic distortion (THD) in output voltage of the inverter is another goal [26]. In the present paper, AFSMC method is introduced to control voltage and frequency in microgrid. In the following, different types of droop control methods including conventional and generalized droop control are described in next section. The generalized droop control method based on adaptive fuzzy-sliding mode is then suggested and it is introduced in the third section. To evaluate performance of the proposed method, the simulation results are then presented. Finally, the paper is concluded in the last section.

Droop Control

A. The conventional droop control

A simple microgrid depicted in Fig. 1 is considered here in which the DG is connected to load through a line with Z impedance. As illustrated from this figure, active and reactive power in S point can be stated as follows:

$$P=\frac{V_S^2}{Z}\cos\vartheta-\frac{V_SV_L}{Z}\cos(\vartheta+\delta) \tag{1}$$

$$Q=\frac{V_S^2}{Z}\sin\vartheta-\frac{V_SV_L}{Z}\sin(\vartheta+\delta) \tag{2}$$

where ϑ is angle related to the line impedance. Considering $Ze^{j\vartheta}=R+jX$, (1) and (2) can be written as follows:

$$P=\frac{V_S}{R^2+X^2}[R(V_S-V_L\cos\delta)+XV_L\sin\delta] \tag{3}$$

$$Q=\frac{V_S}{R^2+X^2}[-RV_L\sin\delta+X(V_S-V_L\cos\delta)] \tag{4}$$

The above equations show that output voltage of inverter and the power angle (δ) depend on active and reactive powers. Assuming $X>>R$ and a very small power angle, we have:

$$\delta=\frac{XP}{V_SV_L}\ ,\quad V_S-V_L=\frac{XQ}{V_S} \tag{5}$$

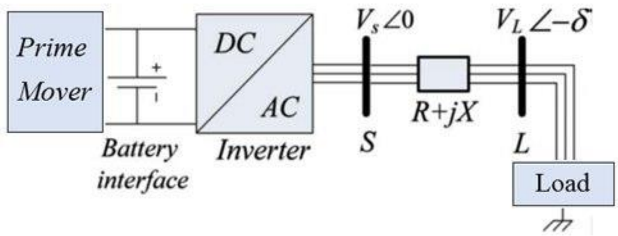

Fig. 1: A simple microgrid with inverter.

With regard to (5), it is illustrated that P must be controlled to regulate δ while V_S can be controlled through Q for an inductive microgrid. In other words, the reactive power controls output voltage of the inverter and active power controls system frequency. These control strategies are known as *Q/V* and *P/f*, respectively. With considering the above issues, two ordinary equations can be defined for controlling *Q/V* and *P/f* with applying linear approximation:

$$f-f_0=-k_p(P-P_0) \tag{6}$$

$$V_S-V_{S0}=-k_q(Q-Q_0) \tag{7}$$

where f_0 and V_{S0} are the rated voltage and frequency of the microgrid, and k_p and k_q are droop coefficients of DG's active and reactive power. With regard to (6) and (7), if inverter's frequency or voltage changes for any reason, this effect can be observed in active and reactive power of inverter output. The appropriate deviation value of frequency and voltage can be obtained through droop characteristics. This primary control provides a quick control action to maintain moment balance between production and consumption. Despite of changes in the frequency index and the pulse wide modulation (PWM) voltage of generator, microgrid voltage and frequency are kept in the nominal range. For a resistant microgrid *(X<<R)*, (5) is modified as follows:

$$\delta=-\frac{RQ}{V_SV_L}\ ,\ V_S-V_L=\frac{PR}{V_S} \tag{8}$$

The relationship between reactive power and power angle and also between active power and voltage are illustrated in (8). By frequency regulation, power angle is controlled automatically. Therefore, in resistant microgrid, droop control techniques of *Q/f* and *P/V* are required to control voltage and frequency, respectively. These methods are based on independency of voltage changes and frequency deviation. It is noted that these two factors (voltage and frequency) are dependent on the line parameters.

B. Generalized droop control

Generally, both *R* and *X* should be considered for the droop control [9]. As a result, the corrected active and reactive powers are stated as follows:

$$P'=\frac{X}{Z}P-\frac{R}{Z}Q \tag{9}$$

$$Q'=\frac{R}{Z}P+\frac{X}{Z}Q \tag{10}$$

With defining K_R equals to R/X and using (6), (7), (9) and (10), the following equations are resulted:

$$P'=\frac{X}{Z}\left[K_f\Delta f+P_0-K_RK_V\Delta V_S-K_RQ_0\right] \tag{11}$$

$$Q'=\frac{R}{Z}P'=\frac{X}{Z}\left[K_RK_f\Delta f+K_RP_0+K_V\Delta V_S+Q_0\right] \tag{12}$$

where $K_f=-1/k_p$, $K_V=-1/k_q$ and Δf and ΔV_S are frequency deviation and inverter voltage, respectively. In (11) and (12), K_R index is defined to show resistance line percentage. This index helps us to understand simultaneous control of voltage and frequency. After performing algebraic calculations on (11) and (12), the following expressions are obtained:

$$\Delta f=\frac{1}{K_f}\left(\frac{Z}{X}P'-P_0\right)+\frac{K_RK_V}{K_f}\Delta V_S+\frac{K_R}{K_f}Q_0 \tag{13}$$

$$\Delta V_s=\frac{1}{K_V}\left(\frac{Z}{X}Q'-Q_0\right)-\frac{K_RK_f}{K_V}\Delta f-\frac{K_R}{K_V}P_0 \tag{14}$$

From (13), it is obvious that K_f influences on weighted coefficients of ΔV_S and Q_0 (the second and third terms, respectively). So, to avoid from unwanted impact of K_f on ΔV_S and Q_0 (in the second and the third terms of (13)), K_f should be selected the unit. Similarly, K_V (in the second and the third terms of (14)) is assumed to be 1. Then, relationship for the generalized droop control (GDC) can be achieved as follows:

$$\Delta f=\frac{1}{K_f}\left(\frac{Z}{X}P'-P_0\right)+K_RK_V\Delta V_S+K_RQ_0 \tag{15}$$

$$\Delta V_s=\frac{1}{K_V}\left(\frac{Z}{X}Q'-Q_0\right)-K_RK_f\Delta f-K_RP_0 \tag{16}$$

The block diagram related to (15) and (16) is depicted in Fig. 2.

Fig. 3 shows the conventional block diagram for a VSI. The LCL output filter is also added to prevent from resonance effect in network output. Also, LCL damps the distortion of output sinusoidal waveform and reduces high frequency harmonic resulted from VSI switching. Therefore, it is used in output of inverter to keep appropriate quality for output current and bus-voltage during connection to a weak network. Active and reactive powers pass from low-pass filter as follow:

$$P'=\frac{\omega_c}{s+\omega_c}P\ ,\ Q'=\frac{\omega_c}{s+\omega_c}Q \tag{17}$$

where ω_c is the cutoff frequency of low-pass filter. The power controller calculates the required active and reactive power and it produces P' and Q' for simultaneous control of voltage and frequency.

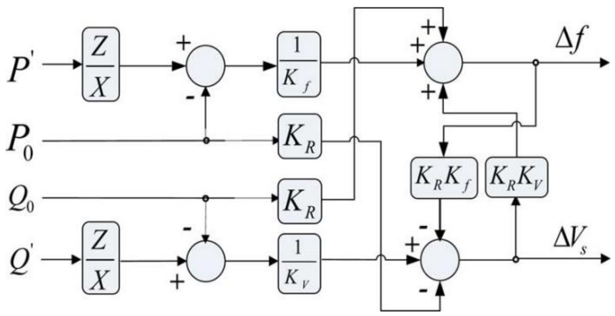

Fig. 2: The GDC block diagram of voltage and frequency control.

The GDC Based on AFSMC

The main weakness point of the GDC method described in previous section is its high dependency to line parameters (*R* and *X*). This matter results in weak performance of the control method in the case of failure to accurately identify the line parameters. Therefore, a new method based on AFSMC is introduced here to eliminate it. In this method, the GDC block with suggested controller which is shown in Fig. 4 is replaced. Hence, the dependency to line parameters is removed. In other words, the most important factor in the proposed method is the non-dependence on line parameters. Therefore, the proposed method can be used for any DG in a microgrid system without the need to identify the microgrid. In this figure, e parameter which is selected as an input for the suggested controller is defined as follows:

$$e_P=P_0-P' \tag{18}$$

$$e_Q=Q_0-Q' \tag{19}$$

The output of controller (u) for e_P and e_Q errors are Δf and ΔV, respectively.

A. Description of sliding mode

Assume that an interconnected power system can be modeled as follows:

$$\dot{x}(t)=f\big(x(t)\big)+Bu(t)+\gamma(t) \tag{20}$$

where $x(t)\in R^n$ and $u(t)\in R^m$ are state and control vectors, $\gamma(t)\in R^n$ is external disturbance, $B\in R^n$ is a fixed matrix. The aim of control is to track x_d command through x state using an appropriate control signal. So, we define:

$$e=x-x_d \tag{21}$$

To design the controller, the first stage is to select a sliding surface defines as follows:

$$s(t)=k_1e(t)+\int_0^t k_2e(\tau)\,d\tau \tag{22}$$

where k_1 and k_2 are constants greater than zero.

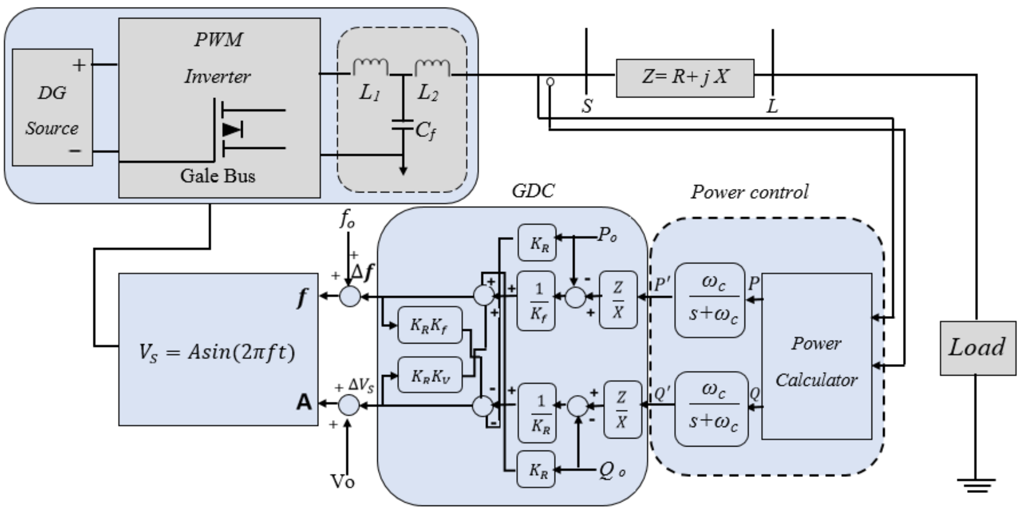

Fig. 3: Microgrid with conventional block diagram for VSI.

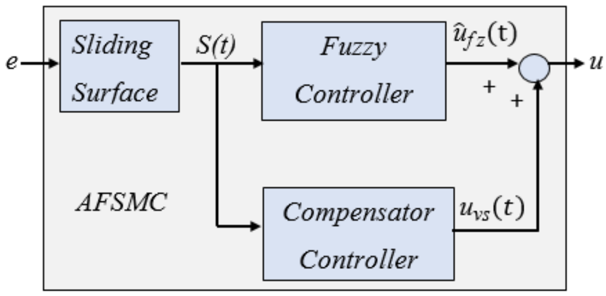

Fig. 4: Suggested controller block diagram.

Assuming that dynamic of system is known, ideal control system can be defined as follows:

$$u^*=\frac{1}{B}[-f(x)+\dot{x}_d-k_1\dot{e}-k_2e-\gamma(t)] \tag{23}$$

With substituting (23) in (1), we will have:

$$\dot{e}+k_1\dot{e}+k_2e=0 \tag{24}$$

With correct selection of k_1 and k_2, (25) shows the Horowitz stable. Since the system dynamic cannot be estimated easily, the law of ideal control of (23) is not applicable. Therefore, the suggested AFSMC is implemented to follow the ideal control law.

B. The AFSMC implementation

With regards to Fig. 4, it can be written:

$$u=\hat{u}_{fz}+u_{vs} \tag{25}$$

where the control rule (u^*) is done through the main tracker controller or the fuzzy controller ($\hat{u}_{fz}$) and the difference among u^* and $\hat{u}_{fz}$ is compensated through the compensator control system (u_{vs}). If α_i is a variable parameter, we will have:

$$u_{fz}(s,\alpha)=\alpha^T\xi \tag{26}$$

where $\xi=[\xi_1, \xi_2,\ldots,\xi_m]$ and $\alpha=[\alpha_1,\alpha_2,\ldots,\alpha_m]$ are parameters and regression vectors that ξ_i is written as follows:

$$\xi_i=\frac{w_i}{\sum_{i=1}^m w_i} \tag{27}$$

where w_i is the weight of ith law. Based on [25], it is possible to write an optimal fuzzy control system ($u_{fz}^*(s,\alpha^*)$) for structure proposed in (26) as follows:

$$u^*(t)=u_{fz}^*(s,\alpha^*)+\varepsilon=\alpha^{*T}\zeta+\varepsilon \tag{28}$$

where ε shows the error of approximation and it is assumed that it is limited by $|\varepsilon|<E$. With applying the considered fuzzy control system to approximate $u^*(t)$, we have:

$$\hat{u}_{fz}(s,\hat{\alpha})=\hat{\alpha}^T\xi \tag{29}$$

where $\hat{\alpha}$ is approximation vector of α^*. With substituting (29) in (30), the following equation is resulted:

$$\ddot{x}(t)=f(x(t))+B[\hat{u}_{fz}+u_{vs}]+\gamma(t) \tag{30}$$

Using (20), (23) and (24), error equation related to the closed loop system can be derived as follows:

$$k_1 e(t)+k_2\int_0^t e(\tau)\,d\tau+k_3\dot{e}(t)=B\left[\hat{u}_{fz}+u_{vs}-u^*\right]=\dot{s}(t) \tag{31}$$

And $\tilde{u}_{fz}$ will be as follow:

$$\tilde{u}_{fz}=\hat{u}_{fz}-u^*=\hat{u}_{fz}-\left[u^*_{fz}+\varepsilon\right] \tag{32}$$

For simplification, $\tilde{\alpha}=\hat{\alpha}-\alpha^*$ to derive new form of (32) from (28) and (29).

$$\tilde{u}_{fz}=\tilde{\alpha}^T\zeta-\varepsilon \tag{33}$$

To make zero $s(t)$ and $\tilde{\alpha}$, the Lypunov function is defined as follows:

$$V_a(t)=\frac{1}{2}s^2(t)+\frac{B}{2\eta_1}\tilde{\alpha}^T\tilde{\alpha} \tag{34}$$

where η_1 is a positive constant. With differentiation from (34), we have:

$$\begin{aligned}\dot{V}_a(t)&=s(t)\dot{s}(t)+\frac{B}{2\eta_1}\tilde{\alpha}^T\dot{\tilde{\alpha}}\\&=s(t)B\left(\hat{u}_{fz}+u_{vs}-u^*\right)+\frac{B}{2\eta_1}\tilde{\alpha}^T\dot{\tilde{\alpha}}\\&=s(t)B\left(\tilde{\alpha}^T\zeta+u_{vs}-\varepsilon\right)+\frac{B}{2\eta_1}\tilde{\alpha}^T\dot{\tilde{\alpha}}\\&=B\tilde{\alpha}^T\left(s(t)\zeta+\frac{1}{\eta_1}\dot{\tilde{\alpha}}\right)+s(t)B(u_{vs}-\varepsilon)\end{aligned} \tag{35}$$

To achieve $\dot{V}_a(t)<0$, how to change the parameters related to the fuzzy controller and output of the compensator controller can be obtained as follows:

$$\dot{\tilde{\alpha}}=\dot{\hat{\alpha}}=-\eta_1 s(t)\zeta \tag{36}$$

$$u_{vs}=-E\,sgn\left(s(t)\right) \tag{37}$$

where *sgn* indicates to the sign function. Then, (35) can be rewritten as follows:

$$\begin{aligned}\dot{V}_a(t)&=-E|s(t)|B-\varepsilon s(t)B\le -E|s(t)|B+|\varepsilon||s(t)|B\\&=-(E-|\varepsilon|)|s(t)|B\le 0\end{aligned} \tag{38}$$

It means that $\dot{V}_a(t)$ is a negative semi-definite function. And,

$$Q(t)=(E-|\varepsilon|)|s(t)|B\le -\dot{V}_a(t) \tag{39}$$

Since $V_a(t)$ is limited and $\dot{V}_a(t)$ is incremental and limited, we have:

$$\int_0^t Q(\tau)\,d\tau\le V_a(t_1)-V_a(t_2)<\infty \tag{40}$$

With regard to the rule of Barbalet introduced in [26], the below condition can be followed:

$$\lim_{t\to\infty} Q(t)=0 \tag{41}$$

In other word, $s(t)\to 0$ when $t\to\infty$. Therefore, stability of the proposed AFSMC can be guaranteed.

Simulation Results

A. Standard power system

In this section, performance of the proposed controller under different conditions of the power system depicted in Fig. 1 is evaluated. Simulation of the considered power system is done to track different values of active and reactive power. If the parameters k_1 and k_2 are selected correctly, desirable dynamic of the system including rise time, overshoot and settling time can be obtained easily. In addition, η_1 and E are selected to achieve to the best transient response with regard to stability constraint and the control output. The controller parameters required for simulation are summarized in Table 1. It must be added that a separate AFSMC controller is used to control active and reactive power.

Table 1: Controller Parameters

Controller	E	k_2	k_1	η_1
Active power controller	12	5000	2	12
Reactive power controller	9	1000	2	9

When changing the reference active power, the generator response for the proposed AFSMC and the discussed SMC controller are obtained and they are compared in Figs. 5 and 6. As it observed in these figures, the speed of the discussed SMC is a little more than the suggested AFSMC but chattering domain in the SMC is about 0.02 pu that is a relative large value. This chattering can affect the power system dynamic, power loss and stability. In contrast, the chattering is so low for the response of microgrid when the suggested AFSMC is applied. In addition, steady-state error for active power in the presence of suggested method is small. In Fig. 6, the frequency of microgrid has been shown for change of active power. It is clear that the performance of the proposed AFSMC controller is much better than the discussed SMC method. In Table 2, dynamic performance of the considered microgrid has been compared for the two controllers. It is observed that the dynamic performance of suggested method is better than the SMC method. Furthermore, THD value in the inverter output voltage is very little in the presence of the suggested method.

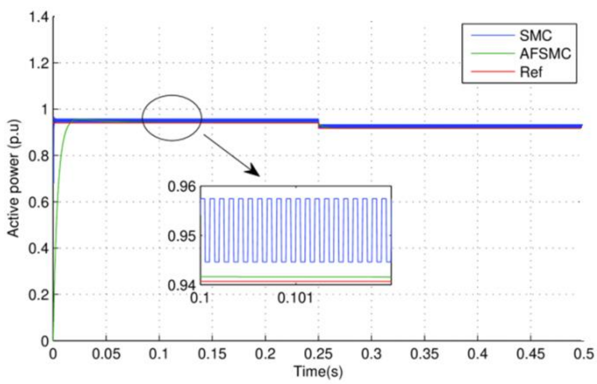

Fig.5: Generator output active power.

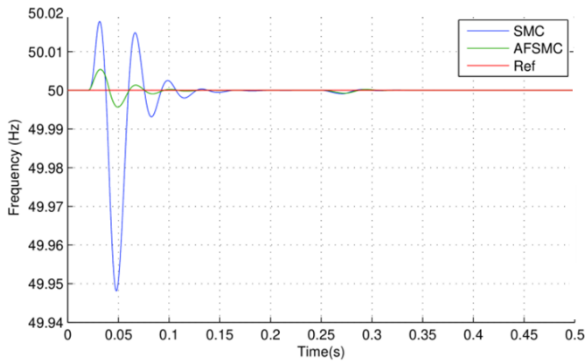

Fig. 6: The microgrid frequency.

Table 2: The dynamic response of different methods

Method	Steady-state error [%]	Settling time [s]	Rise time [s]	THD [%]
SMC	1.64	0.01	0.001	0.91
AFSMC	0.22	0.01	0.005	0.01

For the second case study, it is assumed that the grid voltage is reduced from 1 pu to 0.7 pu in t=0.2s and it is then increased to l pu again at t=0.4s. The active power of generator, microgrid frequency, reactive power and bus voltage have been shown in Figs. 7-10, respectively. With regard to Fig. 7, it is observed that there is a significant value of chattering in microgrid response for the discussed SMC controller. As observed in Fig. 8, the change of network frequency is damped faster using the proposed AFSMC controller. It is also illustrated from Figs. 8 and 9 that the reference active power and reactive power are well tracked by the microgrid. It is clear from Fig. 10 that the bus voltage response of microgrid has significant overshoot for the SMC while there is a satisfactory dynamic response for the suggested AFSMC controller.

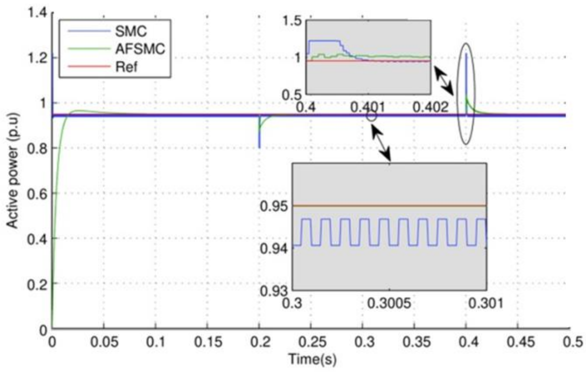

Fig. 7: Generator output active power.

B. *The four-bus four-DG microgrid*

To demonstrate the effectiveness of the suggested secondary controller, a 380 V, 50 Hz four-bus four-inverter-based DG islanded microgrid shown in Fig. 11 is used. All loads and lines are modeled as series RL branches.

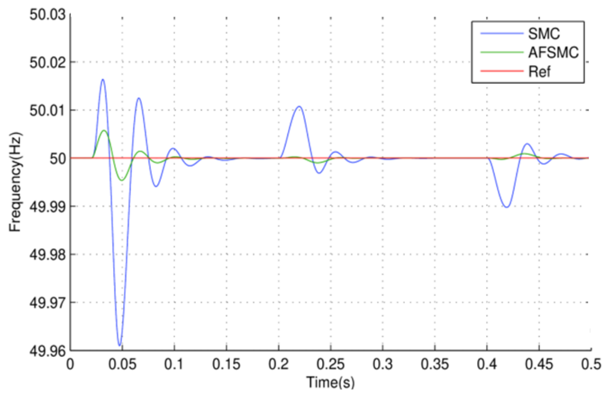

Fig. 8: The microgrid frequency.

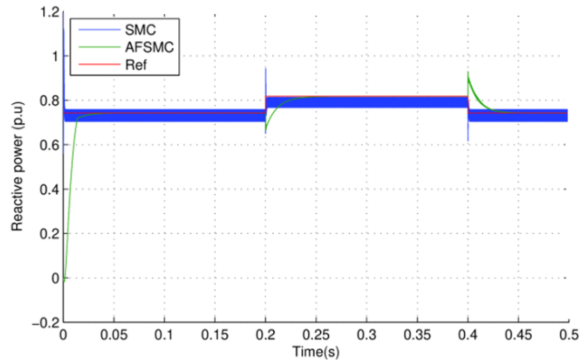

Fig. 9: Generator output reactive power.

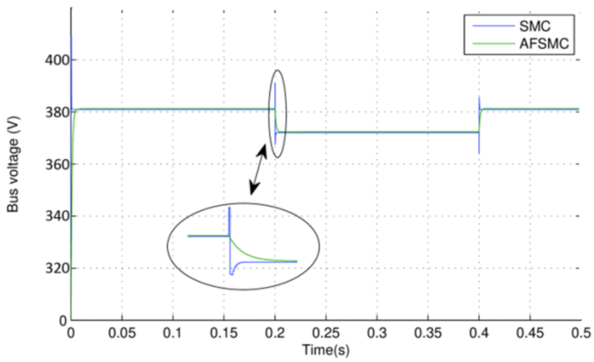

Fig. 10: The microgrid bus voltage.

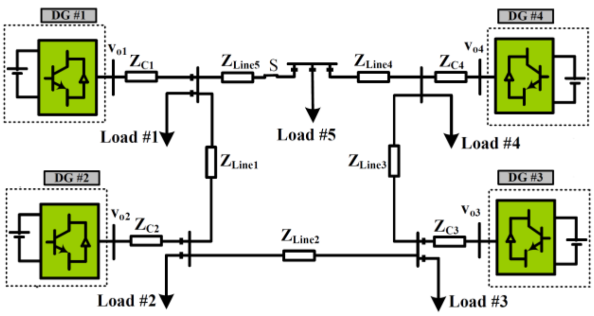

Fig. 11: An islanded four-DG microgrid test system.

The simulation scenario of this part is defined as follows:

1. The proposed secondary control is activated at t=1.5s.

2) Load #1 is increased at t=2s.

3) Load #3 is disconnected at t=3s.

4) Switch S in Fig. 11 is opened at t=3.5s.

In order to show the effective performance of the proposed secondary control, following the process of islanding at t=0s, the proposed secondary control is deliberately disabled. Fig. 12 shows the response of the microgrid such as voltage, frequency, active power and reactive power to the aforementioned fault. As seen in this figure, the terminal voltage of the DGs and the frequency of the microgrid deviate from their nominal values by their droop controller. Hence, the secondary control loop should restore the frequency and voltage of the microgrid. After the activation of the proposed secondary loop controller (i.e. AFSMC) at t=1.5s, the microgrid's voltage and frequency are quickly restored to the nominal values as seen in Figs. 12 (a) and (b). When load#1 is increased at t=2s, the proposed controller shows good tracking and robust performance against the increase of load#1 and exactly restores the voltage and frequency of the microgrid. To highlight the robust performance of the proposed secondary controller, it is assumed load #3 is removed at t=3s. It is clear from Fig. 12 that the suggested secondary controller can restore the microgrid's the voltage and frequency rapidly.

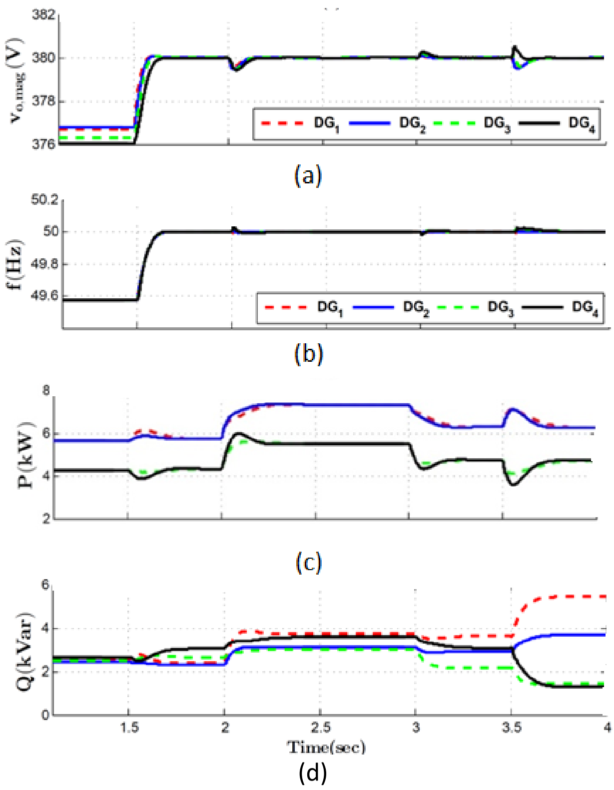

Fig. 12: The response of the microgrid to a multiple fault, (a) terminal voltage of DGs; (b) Frequency of DGs; (c) Active power of DGs; (d) Reactive power DGs

Next, the performance of the proposed controller is evaluated under disconnecting and reconnecting of DGs. For this purpose, DG#4 is disconnected at t=2s and reconnected at t=2.5s. Fig. 13 depicts the response of the microgrid to this fault. After disconnecting DG#4 from the microgrid, the remaining DGs increase power generation to return the amount of power to the generated power before disconnecting. Therefore, the power generation of the remaining DGs increases, while the power generated by DG#4 drops to zero during disconnecting as shown in Fig. 13.c. Besides, at t=2.5s, the process of the synchronization is activated and DG#4 is reconnected to the microgrid. In spite of disconnecting and reconnecting of DG#4 (except for the transient state), AFSMC can also control accurately the voltage and frequency before, during, and after disconnecting and reconnecting as seen from Fig. 13. Here, a comparative study is conducted between the proposed AFSMC and the secondary control loop proposed in [27]. It should be noted that the controller proposed in[27] is an asymptotic controller that ensure the global asymptotic stability of the microgrid. Fig. 14 displays the simulation results for when voltage and the frequency of DG#1 are restored using the two controllers.

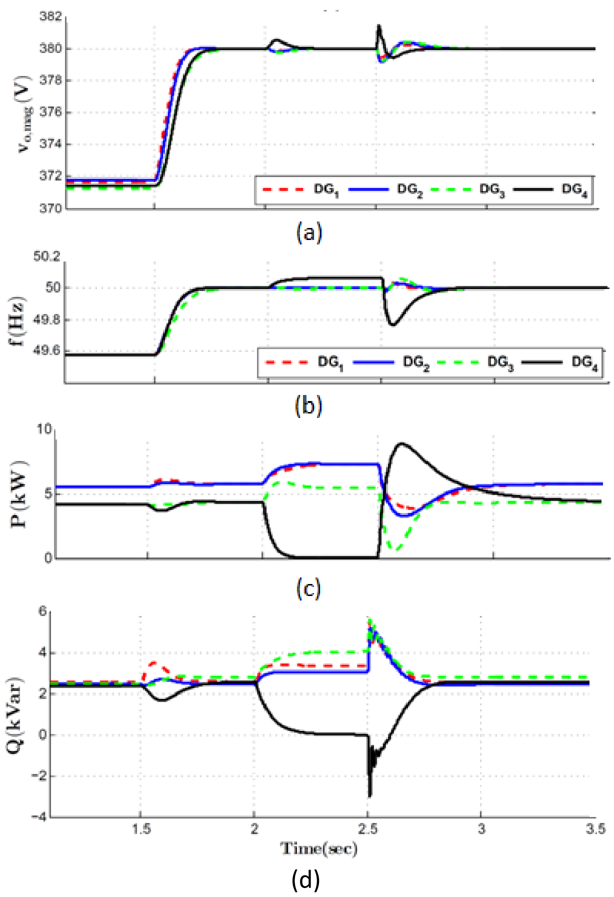

Fig. 13: The response of the microgrid to the disconnecting and reconnecting of DG#4, (a) terminal voltage of DGs; (b) Frequency of DGs; (c) Active power of DGs; (d) Reactive power DGs.

For simplicity, only the frequency response and voltage of the one of DGs are indicated. The results can be concluded: 1) compared to the proposed method in [27], our proposed method quickly reaches to the nominal value and it shows more accurate performance for activating the controller, the reconfiguration of the structure and load variations, 2) the proposed method provides better disturbance rejection properties in the reconfiguration and load variations.

Conclusion

A solution for droop control based on generalized droop control was introduced to regulate simultaneously voltage and frequency in islanded microgrid. A generalized droop control method based on conventional voltage and frequency droop control was presented first but it was shown that this method depends seriously on power system configuration and transmission line parameters. To solve the problem, an independent generalized droop control method was suggested that was independent from the model of the microgrid. The suggested controller simulates the dynamic behavior of the generalized droop control. In this suggested intelligent controller, the abilities of the sliding mode controller and fuzzy controller are combined to introduce an appropriate adaptive controller. In order to ensure the stability of the closed loop system, an effective algorithm based on the Lyapunov stability rule was also established. To reduce the chattering phenomenon, a compensatory controller was used for the suggested controller. This proposed controller was applied to a typical microgrid for control of voltage and frequency. The simulation results showed great ability of the suggested controller to keep micro-grid stability in various conditions.

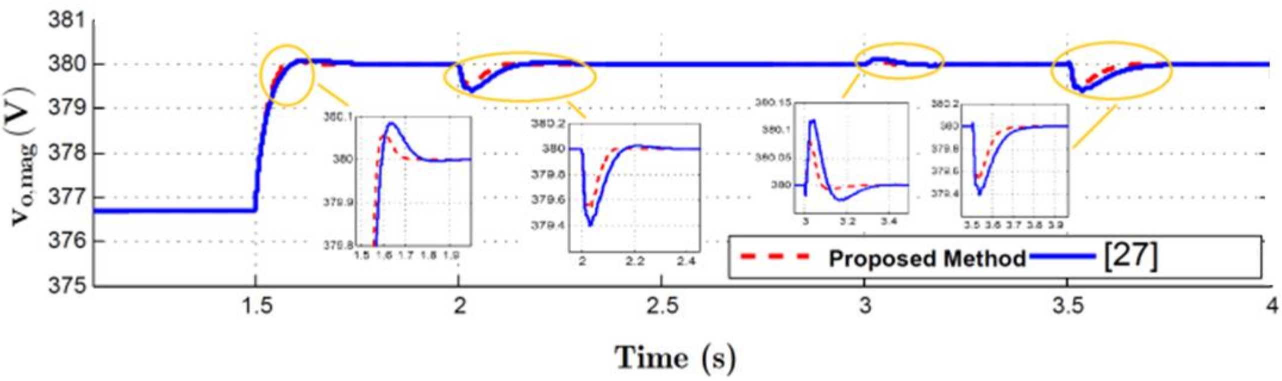

(a)

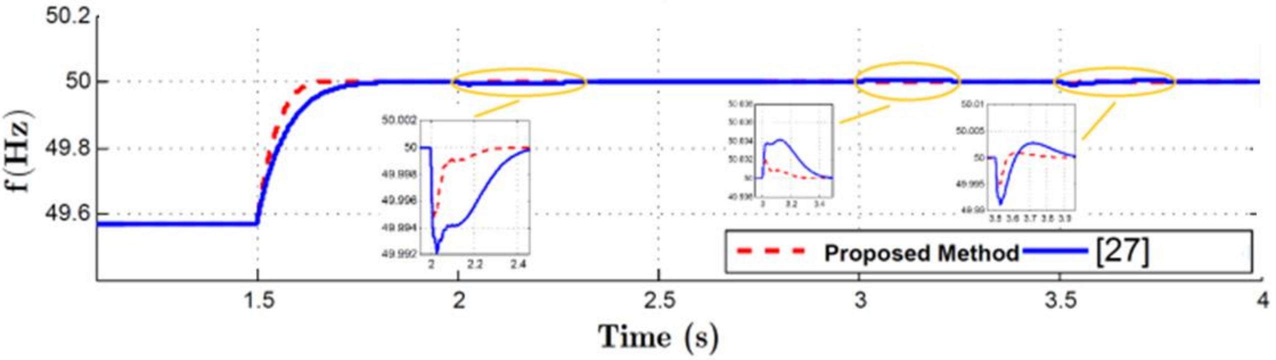

(b)

Fig. 14: The comparative study results.

Author Contributions

The idea of the work was proposed by E. Limouchi, S. A. Taher, and B. Ganji. The simulation model was developed by E. Limouchi and he also carried out the data analysis. S. A. Taher, and B. Ganji interpreted the results and wrote the manuscript.

Acknowledgment

The author gratefully acknowledges the D. O. Amoateng, M. Al Hosani, M. S. Elmoursi, K. Turitsyn, and J. L. Kirtley for their work on the original version of this document.

Conflict Of Interest

The author declares that there is no conflict of interests regarding the publication of this manuscript. In addition, the ethical issues, including plagiarism, informed consent, misconduct, data fabrication and/or falsification, double publication and/or submission, and redundancy have been completely observed by the authors.

Abbreviations

f	Measured frequency
f_o	Standard grid frequency set point
P	Active power output
P_o	Active power set value
V_{abc}	Three-phase voltage
V_α, V_β	Clark voltage
I_{abc}	Three-phase current
V_d, V_q	Park voltage
Q_o	Reactive power set value of the generator
Q	Reactive power output
K_v	Voltage droop setting
K_f	Frequency droop setting
V	Voltage of coupling point

References

[1] R. Kadri, J. P. Gaubert, G. Champenois, "An improved maximum power point tracking for photovoltaic grid-connected inverter based on voltage-oriented control," IEEE Trans. Ind. Electron., 58(1): 66-75, 2011.

[2] H. Bevrani, "Microgrid controls," Standard Handbook for Electrical Engineers, McGraw Hill, 2012.

[3] R. Lasseter, J. Eto, B. Schenkman, J. Stevens, H. Vollkommer, D. Klapp, E. Linton, H. Hurtado, J. Roy, "CERTS microgrid laboratory test bed," IEEE Trans. Power Del., 26(1): 325-332, 2011.

[4] C. Moreira, J. P. Lopes, "Microgrids dynamic security assessment," in Proc. IEEE International Conference on Clean Electrical Power: 26-32, 2007.

[5] J. Hu, J. Zhu, D. G. Dorrell, J. M. Guerrero, "Virtual flux droop method, a new control strategy of inverters in Microgrids, " IEEE Trans. Power Electron., 29(9): 4704-11, 2014.

[6] E. Rokrok, M. Shafie-Khah, J. P. Catalão, "Review of primary voltage and frequency control methods for inverter-based islanded microgrids with distributed generation," Renewable and Sustainable Energy Reviews, 82: 3225-3235, 2018.

[7] M. R. HojatyDana, M. R. AlizadehPahlavani, "Control strategies for performance assessment of an autonomous wind energy conversion system," Journal of Electrical and Computer Engineering Innovations (JECEI), 2(2): 15-20, 2014.

[8] H. Amiri, G. Arab, N. Mahdian, "Voltage control and load sharing in a DC islanded microgrid based on disturbance observer," Journal of Electrical and Computer Engineering Innovations (JECEI), 7(1): 1-10, 2019.

[9] D. O. Amoateng, M. Al Hosani, M. S. Elmoursi, K. Turitsyn, J. L. Kirtley, "Adaptive voltage and frequency control of islanded multi-microgrids," IEEE Trans. Power Syst., 33(4): 4454-4465, 2017.

[10] T. Vigneysh, N. Kumarappan, "Artificial neural network based droop-control technique for accurate power sharing in an islanded microgrid," International Journal of Computational Intelligence Systems, 9(5): 827-838, 2016.

[11] A. Karaki, M. Begovic, S. Bayhan, H. Abu-Rub, "Frequency and voltage restoration for droop controlled AC microgrids", International Conference on Smart Grid and Renewable Energy (SGRE): 1-6, 2019.

[12] P. Subbaraj, K. Manickavasagam, "Generation control of interconnected power systems using computational intelligence techniques," IET GENER TRANSM DIS., 1(4): 557-563, 2007.

[13] H. Bevrani, A. Ghosh, G. Ledwich, "Renewable energy sources and frequency regulation: Survey and new perspectives," IET RENEW POWER GEN., 4(5): 438-457, 2010.

[14] P. Villenueve, "Concerns generated by islanding [electric power generation]," IEEE Power Energy Mag., 2: 49-53, 2004.

[15] J. M. Guerrero, J. C. Vasquez, J. Matas, L. G. de Vicuña, and M. Castilla, "Hierarchical control of droop-controlled AC and DC micro grids-A general approach toward standardization," IEEE Trans. Ind. Electron., 58(1): 158-172, 2011.

[16] S. Peng, A. Luo, Y. Chen, Z. Lv, "Dual-loop power control for single phase grid-connected converters with LCL filter," J. Power Electron., 11(4): 1-8, 2011.

[17] M. Sitbon, S. Schacham, A. Kuperman, "Disturbance observer based voltage regulation of current-mode-boost-converter interfaced Photovoltaic generator," IEEE Trans. Ind. Electron., 62(9): 5776-5785, 2015.

[18] A. G. Yepes, F. D. Freijedo, J. Doval-Gandoy, O. Lopez, J. Malvar, P. Fernandez-Comesana, "Effects of discretization methods on the performance of resonant controllers," IEEE Trans. Power Electron., 25(7): 1692-1712. 2010.

[19] A. Kuperman, "Proportional-resonant current controllers design based on desired transient performance," IEEE Trans. Power Electron., 30(10): 5341-5345, 2015.

[20] C. Kannana, N. K. Mohantyb, R. Selvarasuc, "A new topology for cascaded H-bridge multilevel inverter with PI and Fuzzy control," Energy Procedia, 117: 917-926, 2017.

[21] F. Karbakhsh, G. B. Gharehpetian , J. Milimonfared, A. Teymoori, "Three-phase photovoltaic grid-tied inverter based on feed-forward decoupling control using fuzzy-PI controller," in Proc. IEEE Power Electronics, Drive Systems &Technologies Conf.: 344-348, 2016.

[22] K. Sinthipsomboon, W. Pongaen, P. Pratumsuwan, "A hybrid of fuzzy and fuzzy self-tuning PID controller for servo electro-hydraulic system," in Proc. IEEE Industrial Electronics and Applications Conf.: 220- 225, 2011.

[23] P. Cortes, J. Rodriguez, C. Silva, A. Flores, "Delay compensation in model predictive current control of a three-phase inverter," IEEE Trans. Ind. Electron., 59(2): 1323-132, 2012.

[24] Z. Zeng, H. Li, S. Tang, H. Yang, R. Zhao, "Multi-objective control of multifunctional grid-connected inverter for renewable energy integration and power quality service," IET Power Electron., 9(4): 761-70, 2016.

[25] E. Limouchi, S. A. Taher, B. Ganji, "Active generators power dispatching control in smart grid," in Proc. IEEE Electrical Power Distribution Networks Conf.:26-32, 2016.

[26] S. Xiaoling, and et al., "Microgrid stability controller based on adaptive robust total SMC," Energies, 8: 1784-1801, 2015.

[27] F. Guo, C. Wen, J. Mao, and Y.-D. Song, "Distributed secondary voltage and frequency restoration control of droop-controlled inverter-based microgrids," IEEE Trans. Ind. Electron., 62(7): 4355-4364,. 2015.

Biographies

Ehsan Limouchi was born in Esfahan, Iran, in 1980. He received the M.Sc. degree in Electrical- Control Engineering from Islamic Azad University, Science and Research Branch, Tehran, Iran in 2007. He is currently working toward the Ph.D. degree in Electrical Engineering at University of Kashan. His research interest includes control theory, power electronics and micro grid control systems.

Seyed Abbas Taher (SM'17) was born in Kashan, Iran, in 1964. He received the B.Sc. degree in electrical engineering from the Amirkabir University of Technology, Tehran, Iran, in 1988, and the M.Sc. and Ph.D. degrees in electrical engineering from Tarbiat Modares University, Tehran, in 1991 and 1997, respectively. In 1996, he joined the Faculty of Engineering, University of Kashan, where he has been a Full Professor since 2016. His current research interests include power system optimization and control design, analysis of electrical machines, power quality, and renewable energy.

Babak Ganji was born in Isfahan, Iran, in 1977. He received B.Sc. degree from Isfahan University of Technology, Iran in 2000, and M.Sc. and Ph.D. from University of Tehran, Iran in 2002 and 2009 respectively, all in major electrical engineering-power. He was granted DAAD scholarship in 2006 from Germany and worked in institute of power electronics and electrical drives at RWTH Aachen University as a visiting researcher for 6 months. He has been working at University of Kashan in Iran since 2009 and his research interest is modeling and design of electric machines especially switched reluctance motor.

How to cite this paper:

E. Limouchi, S. A. Taher, B. Ganji "Frequency and Voltage Control of an Inverter-Based DG Using Adaptive Fuzzy-Sliding Mode Controller ," Journal of Electrical and Computer Engineering Innovations, 7(2): 221-230, 2019.

DOI: 10.22061/JECEI.2020.6606.329

URL: http://jecei.sru.ac.ir/article_1371.html